

Morphology and phylogenetic significance of the thoracic muscles in Psocodea (Insecta: Paraneoptera)

Azuma Kawata | Naoki Ogawa | Kazunori Yoshizawa

Systematic Entomology, School of Agriculture, Hokkaido University, Sapporo 060-8589, Japan

Correspondence

Kazunori Yoshizawa, Systematic Entomology, School of Agriculture, Hokkaido University, Sapporo 060-8589, Japan

Email: psocid@res.agr.hokudai.ac.jp

Abstract

The thoracic musculature of the insect order Psocodea has been examined in only a few species of a single suborder to date. In the present study, we examined the thoracic musculature of species selected from all three suborders of Psocodea to elucidate the ground plan of the order and to examine the phylogenetic utility of the character system. The sister-group relationship between the suborders Troctomorpha and Psocomorpha received support from two novel nonhomoplasious synapomorphies, although the support from other morphological characters for this relationship is ambiguous. The sister-group relationship between the infraorders Epipsocetae and Psocetae also received support from one nonhomoplasious synapomorphy, although no other morphological characters supporting this relationship have been identified to date. The present examination revealed the potential of thoracic muscle characters for estimating deep phylogeny, possibly including interordinal relationships.

Keywords: Synchrotron μ CT, higher-level phylogeny, psocopterans, Trogiomorpha, Troctomorpha, Psocomorpha

1 | INTRODUCTION

Psocodea is a hemimetabolous insect order composed of nonparasitic bark and book lice and parasitic lice (de Moya et al. 2021). The order is subdivided into three monophyletic suborders, Trogiomorpha, Troctomorpha (in which parasitic lice are classified), and Psocomorpha. Generally, Troctomorpha and Psocomorpha are considered close relatives (e.g., Mockford 1993; Lienhard 1998), and this relationship has received strong support from molecular data, including genomic data (Yoshizawa et al. 2006; Johnson et al. 2018; de Moya et al. 2021). However, morphological support for these subordinal relationships is limited (Ogawa & Yoshizawa 2018a,b), and additional morphological data are highly desired to corroborate or test the results from molecular and phylogenomic analyses. Conflicts of the phylogenetic signal between the morphological and molecular data were identified in Psocomorpha, but thoracic characters were identified as the most congruent character system with molecular data (Yoshizawa & Johnson 2014).

The thorax of insects houses many muscles. These muscles play important roles in insect locomotion, such as large muscles producing power to flap the wings, mid-sized muscles producing power for leg movement, and fine muscles controlling the movement of the wings and legs (e.g., Maki 1938; Snodgrass 1935; Brodsky 1994). Therefore, these muscles are highly conserved, and most of the thoracic muscles can be homologized throughout the neopteran insects (Friedrich & Beutel 2008, 2010). Such properties of insect thoracic muscles (i.e., many slowly evolving characteristics that can be homologized for a wide variety of insect orders) indicate their potential usefulness in estimating the higher-level phylogenetic relationships of insects, including intra- and inter-ordinal ones.

However, available data on the thoracic muscles of Psocodea are limited. Only a single character selected from a dorso-ventral indirect flight muscle was utilized for the morphological phylogeny of Psocomorpha (Yoshizawa 2002; Yoshizawa & Johnson 2014). Comprehensive morphological examinations have been conducted for only two species of a single suborder, Psocomorpha (Maki 1938; Badonnel 1934). The systematic placement of Psocodea has become an actively debated subject; although Psocodea has long been regarded as a member of Paraneoptera (a super-order composed of Psocodea, Thysanoptera, and Hemiptera: Yoshizawa & Saigusa, 2002; Yoshizawa & Lienhard, 2016), recent phylogenomic analyses suggest a close relationship between Psocodea and Holometabola (Misof et al. 2014; Johnson et al. 2018). Therefore, information on the thoracic musculature of the wide variety of Psocodea and an estimation of its ancestral condition should provide useful information for elucidating the phylogenetic placement of Psocodea.

In this study, we investigated the thoracic musculature of a wide variety of nonparasitic Psocodea species (previously known as an independent insect order “Psocoptera”: we use the term psocopterans to indicate the nonparasitic members of Psocodea in the following sections) selected

from all three suborders. We also performed parsimonious mapping of the thoracic character dataset on the molecular/phylogenomic tree to examine the utility of this character system for estimating the deep phylogeny (infra- and subordinal level) of Psocodea.

2 | MATERIALS AND METHODS

The thoracic musculature of the fully winged species selected from major lineages of nonparasitic Psocodea (psocopterans) were examined. The species examined are listed in Table 1. Samples were either fixed with 80% ethanol or FAA solution (formalin:alcohol:acetic acid = 6:16:1) and then preserved in 80% ethanol. Samples were dehydrated in ascending order with 80–100% ethanol before drying them at the critical point (EM CPD300, Leica, Wetzlar, Germany) to remove water without serious organ shrinkage. Samples were then scanned using synchrotron μ CT at the BL47XU (Uesugi et al. 2012) beamline of the Super Photon ring-8 GeV (SPring-8; Hyogo, Japan) using a stable beam energy of 8 keV in absorption-contrast mode. The tomography system consisted of a full-field X-ray microscope with Fresnel zone plate optics (Uesugi et al. 2017). We used semiautomatic segmentation algorithms based on gray-value differences in ITK-SNAP software (Yushkevich et al. 2006) to obtain 3D-representations of the thoracic musculature.

μ CT-scanning images were unavailable for the infraorder Psocetae so that scanning images of the thoracic muscles of a species of this infraorder (Psocidae: *Trichadenotecnum circularoides*) were obtained using confocal laser scanning microscopy (Leica TCP-SP5; Leica Microsystems, Wetzlar, Germany) with the specimen mounted on a large cover glass (22x24 mm) using glycerol. We used an excitation wavelength of 405 nm and emission wavelength of 480–580 nm for CLSM observation. The 3D-representation of the thoracic musculature was reconstructed using ITK-SNAP.

The phylogenetic significance of thoracic muscle morphology was tested by parsimonious mapping of the thoracic musculature data matrix on a molecular/phylogenomic tree (Yoshizawa et al., 2006; Yoshizawa & Johnson, 2014; de Moya et al., 2021). The software MacClade 4.0 (Maddison & Maddison, 2001) was used for the most parsimonious reconstruction. We also compared the result with the most parsimonious tree estimated by PAUP* 4.0a168 (Swofford, 2002). Outgroup data (Table 1) were either selected from the literature (Polyneoptera and Holometabola from Friedrich & Beutel 2008, 2010; also Czihak 1953 and Maki 1936 for supplementary information of Megaloptera) or newly obtained from the μ CT-images scanned here (Hemiptera: Aphididae: winged morph of *Mindarus japonicus* Takahashi).

3 | RESULTS

The psocopteran thoracic muscles recovered by the present examinations were homologized and

listed according to Friedrich & Beutel (2008, 2012). The sites of origin and insertion of each muscle are indicated by O and I, respectively.

3.1 | Prothorax (Figure 1)

3.1.1 | Dorsal Longitudinal Muscles

Idlm1 (Figure 1a) is a long and rather thin muscle. O: lateral part of prothorax; I: middle of dorsal occipitale.

Idlm2 (Figure 1a) is a long and very thin muscle. O: center of prothorax; I: middle of dorsal occipitale, very close to I of Idlm1.

Idlm5 (Figure 1b) runs parallel with the posterior half of Idlm1, thicker than the latter. O: center of anteroventral margin of pronotum; I: prothorax, very close to O of Idlm1.

3.1.2 | Dorsoventral Muscles

Idvm1 (Figure 1d) is long but rather thin muscle, flattened dorsally. O: anterior end of lateral cervical sclerite; I: dorsal margin of occipitale.

Idvm2 (Figure 1d) consists of two bundles. O: posterior part of lateral cervical sclerite; I: dorsal part of occipitale, very close to I of Idvm1.

Idvm4 (Figure 1b). O: anterodorsal margin of pronotum; I: anterior part of lateral cervical sclerite, close to O of Idvm1.

Idvm10 (Figure 1g) is a thin muscle. O: tip of profurcal arm; I: anterodorsal corner of mesothoracic anepisternum, very close to O of Idlm1.

Idvm15 (Figure 1c) is a long and rather thick muscle tapering ventrally. O: central part of pronotum; I: anterior coxal rim.

Idvm16 (Figure 1b) is a thick muscle composed of two twisted bundles. O: central part of pronotum, just medial to O of Idvm15; I: posterior coxal rim.

Idvm17 (Figure 1e) is a long muscle. O: lateral part of pronotum, lateral to O of Idvm15; I: posterolateral coxal rim.

Idvm18 (Figure 1f) is a thin muscle, running parallel with the ventral half of Idvm17. O: posterior margin of lateral pronotum; I: posterolateral coxal rim, between I of Idvm16 and Idvm17.

Idvm19 (Figure 1d) is a thick and long muscle, largest among the prothoracic muscles. O: lateral region of pronotum, lateral to O of Idvm17; I: trochanteral tendon.

3.1.3 | Pleural Muscles

Itpm1 (Figure 1e) is a short and rather thin muscle. O: dorsolateral part of occipitale; I: dorsal side of base of pleural arm.

Itpm3 (Figure 1e) is a short but thick muscle. O: anterior margin of pronotum, lateral to O of Idvm4; I: dorsal side of base of pleural arm, very close to I of Itpm1.

Ispm2 (Figure 1g) is a very thin muscle. O: prospina; I: anterior region of meso-basalare.

Ipcm2 (Figure 1a) is a long diagonally arranged muscle. O: anterior coxal ridge; I: lateral cervical sclerite of opposite side, close to I of Idvm4.

Ipcm5 (Figure 1f) is a short but thick muscle composed of multiple bundles, dorsally broadened. O: ventral side of base of pleural arm; I: anterior coxal ridge, very close to I of Idvm15.

Ipcm8 (Figure 1g) is a long muscle, running parallel with ventral 2/3 of Idvm19. O: dorsal margin of prothoracic episternum; I: trochanteral tendon, anterolateral to I of Idvm19.

3.1.4 | Sternal Muscles

Iv1m3 (Figure 1a) consists of two bundles. O: anterior surface of tip of profurcal arm; I: ventral part of occipitale.

Iv1m4 (Figure 1g,i) is a transversally arranged muscle, tapering toward insertion position. O: internal surface of dorsal projection of profurcal arm; I: prospina.

Iv1m6 (Figure 1a) is a rather thin muscle. O: posterior surface of dorsal projection of profurcal arm; I: between mesofurcal arm.

Iv1m7 (Figure 1a) is almost the same with length and thickness with Iv1m6. O: posterior surface of dorsal projection of profurcal arm, dorsal to O of Iv1m6; I: anterior part of mesofurcal arm.

Iv1m9 (Figure 1a) is a very thin muscle. O: prospina; I: between mesofurcal arm, central to I of Iv1m6.

Iscm2 (Figure 1i) is a thin and short muscle. O: ventrolateral surface of profurcal arm; I: anterior coxal rim, lateral to I of Idvm15.

Iscm4 (Figure 1i) is a thin and short muscle. O: lateral surface of profurcal arm; I: lateral coxal rim, close to articulation point.

Iscm5 (Figure 1g, i) is a thin but rather long muscle. O: prospina; I: posterior coxal rim.

Iscm6 (Figure 1i) consists of two thin bundles. O: ventral side of profurcal arm (two sites); I: trochanteral tendon, as with Idvm19 and Ipcm8.

Iscm7 (Figure 1a) is a very thin muscle. O: prospina; I: anterior mesocoxal rim.

3.2 | Mesothorax (Figure 1)

3.2.1 | Dorsal Longitudinal Muscles

Ildlm1 (Figure 1a) is the thickest mesothoracic muscle composed of multiple bundles. O: large area of anterior lobe of mesoscutum; I: center of mesophragma.

Ildlm2 (Figure 1b) a thick muscle composed of two bundles. O: posteromedial part of mesonotum; I: mesophragma, lateral to I of Ildlm1.

3.2.2 | Dorsoventral Muscles

Ildvm1 (Figure 1d) is (when present) long and thick muscle. See below for observed variation. O: anterior region of lateral lobe of mesoscutum; I: precoxal bridge.

Ildvm2 (Figure 1c) is a long muscle but thinner than Ildvm1, when the latter presents. See below for observed variation. O: anterior region of lateral lobe of mesoscutum, its relative position to Ildvm1 variable among taxa examined; I: trochantin.

Ildvm4 (Figure 1c) is a twisted thick and long muscle consists of two bundles, dorsally flattened. O: posterior region of lateral lobe of mesoscutum, along anterior to lateral margin of O of Ildlm2; I: posterior mesocoxal rim.

Ildvm5 (Figure 1d) is the thinnest among the mesothoracic dvm muscles. O: posterior region of lateral lobe of mesoscutum; I: posterior mesocoxal rim (an exact insertion point was not clearly observable in some species).

Ildvm6 (Figure 1f) is a twisted very thick and long muscle composed of two bundles. O: subalare; I: posterior mesocoxal rim, lateral to I of Ildvm4.

Ildvm7 (Figure 1d) is a long and thick muscle composed of three bundles. O: middle of lateral lobe of mesoscutum, posterior to O of Ildvm1/2; I: trochanteral tendon.

3.2.3 | Pleural Muscles

Iitpm1 (Figure 1e, h) is a small muscle. See below for observed variation. O: base of prealar arm; I: anterodorsal edge of anepisternum.

Iitpm2 (Figure 1e, h) is a small muscle. See below for observed variation. O: base of prealar arm, anterior to O of Iitpm1; I: base of pleural wing process.

Iitpm4 (Figure 1h) is a small muscle. O: pleural arm; I: proximal margin of first axillary sclerite.

Iitpm6 (Figure 1g) is a thin muscle. O: near ventral end of pleural ridge; I: posterior notal wing process.

Iitpm9 (Figure 1h) is a rather well developed, fan-shaped muscle broadly expanded anteroventrally. O: pleural arm, posterodorsal to O of Iitpm4; I: anterior arm of third axillary sclerite.

Iisp1 (Figure 1f) is (when present) a thick muscle. See below for observed variation. O: dorsal

part of anepisternum, including anterior part of basalare; I: lateral region of precoxal bridge, lateral to I of IIdvm1.

IIspm2 (Figure 1j) is (when present) a long but very thin muscle. See below for observed variation.

O: tip of mesofurcal arm; I: mesopleural arm, ventral to O of IItpm9.

IIspm6 (Figure 1g) is a thin, flattened muscle. O: tip of mesofurcal arm, posterointernal to O of IIspm2; I: anterior margin of metanepisternum.

IIpem2 (Figure 1f) is a thick muscle broadened ventrally. O: basalare, posterior to O of IIspm1; I: anterior mesocoxal rim.

IIpem3 (Figure 1f) is a thick muscle broadened ventrally, running parallel with IIpem2. O: basalare, posterior to O of IIpem2; I: anterolateral mesocoxal rim, posterior to I of IIpem2.

IIpem5 (Figure 1e) is a thick and long muscle composed of two bundles. O: basalare, lateral to O of IIspm1, anterior to O of IIpem2; I: trochantral tendon.

3.2.4 | Sternal Muscles

IvIm3 (Figure 1a) is a very short muscle. O: posteroventral margin of mesothoracic furcal arm; I: anterior tip of metathoracic furca.

IIsclm2 (Figure 1j) is a thin, flattened muscle. O: ventrolateral side of base of mesofurcal arm; I: posterior mesocoxal rim, close to I of IIdvm4.

IIsclm4 (Figure 1j) is a long but thin, flattened muscle. O: tip of mesofurcal arm, ventral to O of IIspm2; I: lateral mesocoxal rim close to articulation point.

IIsclm6 (Figure 1j) is a flat muscle. O: dorsolateral part of mesofurca, ventrolateral to I of IvIm7; I: trochantral tendon, internal to I of IIdvm7.

IIsclm7 (Figure 1j) is a thin, flattened muscle. O: posteroventral surface of mesofurcal arm, ventral to O of IvIm3; I: anterior metacoxal rim.

3.3 | Metathorax (Figure 1)

3.3.1 | Dorsal Longitudinal Muscles

IIIdlm1 (Figure 1a) is a thick muscle consists of 4 or 5 bundles. O: near center of mesophragma; I: metaphragma.

IIIdlm2 (Figure 1b,h) is a thick muscle. O: central part of lateral lobe of metascutum; I: metaphragma, lateral to I of IIIdlm1.

3.3.2 | Dorsoventral Muscles

III dvm2 (Figure 1c) is a thick and long muscle. O: anterocentral part of lateral lobe of metascutum; I: trochantin.

III dvm5 (Figure 1e) is a long muscle, possibly consist of one or two bundles, but their distinction is very obscure. O: posterolateral region of lateral lobe of metanotum; I: posterior metacoxal rim.

III dvm6 (Figure 1f) is a thick and long muscle composed of two twisted bundles. O: sabalare; I: posterior metacoxal rim, very close to I of III dvm5.

III dvm7 (Figure 1d) is a thickest metathoracic muscle composed of three bundles. O: median region of lateral lobe of metascutum, anterior to O of III dvm5 and posterolateral to O of II dvm2; I: trochanteral tendon.

III dvm8 (Figure 1j) is tapering toward the origination position. O: anterolateral surface of metafurcal arm, central to O of II vlm3; I: ventrolateral part of metaphragma.

3.3.3 | Pleural Muscles

III tpm2 (Figure 1h) is a small, fan-shaped muscle. O: base of prealar sclerite; I: pleural arm.

III tpm4 (Figure 1h) is a small muscle. O: pleural arm, next to I of III tpm2; I: proximal margin of first axillary sclerite.

III tpm9 (Figure 1h) is a small muscle. O: pleural arm, next to O of III tpm4; I: anterior arm of third axillary sclerite.

III pcm1 (Figure 1g) is tapering ventrally. O: dorsal part of anepisternum; I: trochantin, anterior to I of III dvm2.

III pcm2 (Figure 1f) is along and thick muscle. O: middle of basalare; I: lateral metacoxal rim.

III pcm3 (Figure 1f) runs parallel to III pcm2 and their distinction is rather obscure. It is about the same size with II pcm2 but is tapering dorsally. O: basalare, posterior to O of III pcm2; I: metacoxal rim, posterior to I of III pcm2.

III pcm4 (Figure 1g) is a long but very thin muscle. O: dorsal region of epimeron; I: lateral coxal rim.

III pcm5 (Figure 1e) is a thick and long muscle composed of two bundles. O: anterior part of basalare, anterior to O of III pcm2; I: trochanteral tendon.

III pcm7 (Figure 1k) is (when presents) a short muscle. O: anteroventral edge of metanepisternum; I: posterior mesocoxal rim.

3.3.3 | Sternal Muscles

III scm2 (Figure 1j) consists of three bundles. O: posterolateral surface of metafurcal arm, posterior to O of III dvm8; I: three positions of posterior metacoxal rim.

IIIscm6 (Figure 1j) is a flat muscle. O: anteroventral margin of metafurcal arm; I: trochanteral tendon, anterior to I of IIIIdvm7.

3.4 | Variation within the order

The thoracic musculature is quite consistent throughout the order but some variations were detected among the species examined.

IIdlm1 consists of six or seven bundles per side, and the arrangement of the muscle fibers varies among taxa. However, the number and arrangement can even vary between different sides of the same individual, which may be an artifact caused by dehydration.

IIdvm1 and IIdvm2 vary in number, shape, and arrangement among taxa (Figure 2). In Trogiomorpha, IIdvm1 consists of two bundles, IIdvm2 consists of a single bundle, and IIdvm2 originates central to IIdvm1; in Troctomorpha, IIdvm1 is absent, and IIdvm2 consists of a single bundle; in Archipsocetae, IIdvm1 consists of two bundles, IIdvm2 consists of a single bundle, and IIdvm2 originates external to IIdvm1; in Caeciliusetae and Philotarsetae, IIdvm1 consists of two bundles, IIdvm2 consists of a single bundle, and IIdvm2 originates external to IIdvm1; in Epipsocetae, IIdvm1 consists of a single bundle, IIdvm2 consists of two bundles; and IIdvm2 originates posterior to IIdvm1; and in Psocetae, IIdvm1 is absent and IIdvm2 consists of two bundles.

IItpm1 is observed in most species examined but varies in shape: cylindrical in Trogiomorpha and Troctomorpha (Figure 3a), but fan-shaped in Psocomorpha. IItpm1 is absent in Archipsocetae (Figure 3c, d).

The number of IIIIdvm2 muscle bundles varies from 0 to 2 between species: absent in Lepidopsocidae and Amphientomidae, with a single bundle in Prionoglarididae and two bundles in Psocomorpha.

IItpm2 muscle is cylindrical in shape in Trogiomorpha and Troctomorpha (Figure 3a), whereas it narrows posteriorly in Psocomorpha (Figure 3c). The shape of IIIItpm2 also differs among species, and the variation occurs in parallel with that of the metathoracic IItpm2.

The IIspm1 muscle is absent in Troctomorpha and Psocomorpha but is present in Trogiomorpha and outgroups.

The IIspm2 muscle is observed in *Prionoglaris* and all employed outgroup taxa but absent in all other psocopterans.

IIIpcm5 could not be identified from the scanned data of Lepidopsocidae, but whether this muscle is absent in this taxon or just indistinguishable from IIIpcm2 in this minute species remains uncertain.

IIIpcm7 is observed in Troctomorpha and Psocomorpha but absent in Trogiomorpha.

3.5 | Phylogenetic significance of thoracic muscles

Based on the above observations, the following characters were coded and reconstructed on a molecular/phylogenomic tree (Yoshizawa et al. 2006; Yoshizawa & Johnson, 2014; de Moya et al. 2021) to examine the phylogenetic utility of the character system. Relationships among the outgroups followed Misof et al. (2014), but the monophyly of Paraneoptera was employed because of the instability of the phylogenomic results (Johnson et al. 2018) and consistent morphological support for this superorder (Yoshizawa & Lienhard 2016). Data matrix is available as supplementary online material.

- Character 1. **Ildvm1**, presence/absence (Figure 2): (0) absent; (1) present. This muscle is inserted into the precoxal bridge and present in most psocopteran and outgroup taxa. However, it is absent in Lepidopsocidae (Trogiomorpha: Atropetae), Amphientomidae (Troctomorpha), and Psocidae (Psocomorpha: Psocetae) (Figure 2).
- Character 2. **Ildvm1**, number of bundles: (1) 1; (2) 2 (Figure 2). When the muscle is absent, “?” is coded (see Character 1). The state of this character could not be detected for Megaloptera. The muscle consists of two bundles in most psocopterans, as well as Zoraptera and Aphididae, whereas the muscle consists of only a single bundle in Epipsocidae (Psocomorpha: Epipsocetae).
- Character 3. **Ildvm2**, presence/absence (Figure 2): (0) absent; (1) present. This muscle is absent only in Aphididae (outgroup).
- Character 4. **Ildvm2**, number of bundles (Figure 2): (1) 1; (2) 2. This muscle is inserted into the trochantin in psocopterans. Most psocopteran species, including Zoraptera and Aphididae, consist of a single bundle, but in Epipsocidae (Epipsocetae) and Psocidae (Psocetae) (both Psocomorpha), it is composed of two bundles (Figure 2). The state of this muscle is unknown for Megaloptera.
- Character 5. **Ildvm1** vs. **Ildvm2**, position of origins (Figure 2): (0) Ildvm1 originates external to Ildvm2; (1) Ildvm1 originates medial of Ildvm2. As mentioned above (Characters 1 and 4), the dorso-ventral muscle inserted into the precoxal bridge was interpreted here as Ildvm1, whereas that inserted into the trochantin was interpreted as Ildvm2. When one of these muscles is absent, “?” is coded for this character. The position of their origin varies among taxa. Ildvm1 originates internally from Ildvm2 in Archipsocidae (Psocomorpha: Archipsocetae) and the outgroups, whereas the condition is reversed in Prionoglarididae (Trogiomorpha: Prionoglaridetae), Caeciliusidae (Caeciliusetae), Pseudocaeciliidae (Philotarsetae), and Epipsocidae (Epipsocetae) (all Psocomorpha)

(Figure 2).

- Character 6. **IItpm1**, presence/absence (Figure 3): (0) absent; (1) present. This muscle is absent only in Aphididae (outgroup) and Archipsocidae (Psocomorpha: Archipsocetae).
- Character 7. **IItpm1**, number of bundles (Figure 3). This muscle consists of a single bundle in Psocomorpha except for Archipsocidae (IItpm1 absent in this taxon: see Character 6) and the outgroup (state of this character is unknown for Mecoptera), whereas it is composed of two bundles in Trogiomorpha and Amphientomidae (Troctomorpha).
- Character 8. **IItpm1**, shape (Figure 3): (0) cylindrical; (1) fan shape, broadened anteriorly. State 1 was observed in Trogiomorpha and Amphientomidae (Troctomorpha), whereas the others, including the outgroups showed state 0 (0/1 was given for Megaloptera according to Maki, 1936 and Czihak, 1953).
- Character 9. **II/IIItpm2**, shape (Figure 3): (0) cylindrical (Figure 4a); (1) fan shape, broadened anteriorly (Figure 4c). State 1 is observed in Psocomorpha and Aphididae (outgroup), whereas others show state 0. The change in meso- and metathoracic tpm2 occurs in parallel so that changes in both muscles are coded as a single character.
- Character 10. **IItpm5**, presence/absence: (0) absent; (1) present. This muscle was not observed in psocopterans and zorapterans, but existed in holometabolans (Friedrich & Beutel 2008) and Aphididae.
- Character 11. **IIspm1**, presence/absence (Figure 4): (0) absent; (1) present. The muscle is absent in Troctomorpha and Psocomorpha but is present in Trogiomorpha and outgroups.
- Character 12. **IIspm2**, presence/absence (Figure 5ab): (0) absent; (1) present. This muscle is observed in *Prionoglaris* and all employed outgroup taxa but absent in all other psocopterans.
- Character 13. **IIIpcm7**, presence/absence (Figure 5cd): (0) absent; (1) present. This muscle is observed in Troctomorpha and Psocomorpha but absent in Trogiomorpha and all outgroup taxa.

The maximum parsimony analysis of the thoracic muscle character dataset alone yielded twelve equally parsimonious trees (length = 21) (the outgroup relationships were constrained according to Misof et al., 2014 because no characters informative for resolving the outgroup relationships were selected: see also Materials and Methods). Their strict consensus tree showed completely unresolved, comb-like structure (supplementary online material).

The parsimonious mapping of the dataset on the molecular/phylogenomic tree (Figure 6: length = 22) recovered that Characters 11:0 (absence of II/IIIspm1) and 13:1 (presence of IIIpcm7) (both nonhomoplasious) supported the sister group relationship between Troctomorpha and

Psocomorpha. Character 9:1 (fan-shaped II/IIItpm2) supported the monophyly of Psocomorpha, but the independent occurrence of this character state was also identified in Aphididae (Hemiptera: outgroup). Character 4:2 (IIdvm2 consists of two bundles: nonhomoplasious) provided support for the sister group relationship between Epipsocetae and Psocetae. Character 1:0 (absence of IIdvm1) was identified to evolve independently three times within Psocodea. Character 6:0 (absence of IItpm1) was identified in Archipsocetae and in Aphididae (outgroup). Other characters were more or less homoplasious and could not be reconstructed unambiguously. The consistency index was 0.59, and the retention index was 0.70.

4. | DISCUSSION

4.1 | Homology of the muscles

The thoracic musculature of psocopterans is less variable, and the homology of each thoracic muscle can be identified confidently throughout the species examined here. However, some ambiguities remain in homologization between the psocopterans and other neopteran thoracic muscles as proposed by Friedrich & Beutel (2008).

The origination and insertion positions of the muscle identified here as Ivlm6 is almost identical to that of Ivlm7 *sensu* Friedrich & Beutel (2008), but as described above, the muscle corresponding to Ivlm7 *sensu* Friedrich & Beutel (2008) is clearly seen in Psocodea (Figure 1A). In the neopteran ancestral condition, Ivlm6 is inserted into mesospina, but mesospina is absent in Psocodea (Yoshizawa, 2005). Among the other candidate muscles, the condition of Ivlm6 *sensu* Friedrich & Beutel (2008) is most similar to the muscle here identified as Ivlm6.

The IIscm7 muscle *sensu* Friedrich & Beutel (2008) is defined to originate from the mesospina, but the mesospina is absent in psocopterans. As discussed for Ivlm6, a shift of the origin from the mesospina to the mesofurca is the most likely explanation that occurred according to the loss of the mesospina. Therefore, the muscle that originates from the mesofurca and is inserted into the metacoxa is identified here as IIscm7.

The muscle E of Badonnel (1934) was interpreted as a single muscle but is composed of two bundles (as also illustrated in Badonnel, 1934: fig. 51). The muscle was interpreted as IIpcm3 by Friedrich & Beutel (2008) but is interpreted here as a composition of IIpcm2 (anterior bundle) and 3 (posterior).

The IIIpcm4 muscle *sensu* Friedrich & Beutel (2008) is define to originate from the episternum. However, judging from its relation to the other muscles (IIIIdvm6 and IIIpcm2/3) and insertion position (lateral coxal rim), the muscle originating from the dorsal region of epimeron is identified here as IIIpcm4 of the psocopterans.

The results of our observations agreed well with previous studies (observation made by Badonnel, 1934; Maki, 1938: Table 2). In contrast, there are some incongruences between the present and previous observations (Badonnel, 1934; Maki, 1938) and interpretations by Friedrich & Beutel (2008).

As shown in Table 2, some muscles were not observed by Badonnel (1934) and/or Maki (1938). Most of them are tiny muscles not easily observable even with the μ CT-technique. Therefore, these muscles were probably overlooked by Badonnel (1934) and/or Maki (1938). However, lack of the following muscles was identified to be phylogenetically relevant condition that evolved within Psocodea: Iitpm1, Iispm1, and Iispm2 were not observed in *Stenopsocus* by Badonnel (1934) and/or *Psocus* by Maki (1938) but are observed in many psocopteran. The absence of these muscles in *Stenopsocus/Psocus* is interpreted to be a derived condition that evolved within Psocodea. For the evolutionary pattern and phylogenetic significance of these muscles, see the discussion under Section 4.2.

For some muscles observed by Badonnel (1934), the present examinations using the μ CT technique provided much clearer information about the origination/insertion positions of the following muscles, by which we reached different conclusions from Friedrich & Beutel (2008: supplement 2).

The muscle U of Badonnel (1934) was interpreted as Iidvm8 by Friedrich & Beutel (2008) but was interpreted here as Iispm6. Iidvm8 is the muscle originating from the mesofurca and inserted into the mesophragma. However, our present examination revealed that the muscle U is actually inserted into the metanepisternum, close to the lateral end of the mesophragma, and this condition corresponds to the definition of Iispm6 rather than Iidvm8 *sensu* Friedrich & Beutel (2008).

The muscle e' of Baconnel (1934) was interpreted as Iipcm4 by Friedrich & Beutel (2008) but was interpreted here as Iipcm5, which was interpreted as absent by Friedrich & Beutel (2008). Our present examination clarified that the muscle e' originates from the basalare, which agrees with the definition of Iipcm5 *sensu* Friedrich & Beutel (2008).

In the psocopteran metathorax, there is only a single sclerite between the meso- and metacoxae (Badonnel, 1934; Cope, 1940; Yoshizawa, 2005) which articulates apically with metacoxa. Therefore, the sclerite should be interpreted as the trochantin, and the metathoracic precoxal bridge is undeveloped (Yoshizawa, 2005). Although the metathoracic dorsoventral indirect flight muscle (muscle K of Badonnel, 1934) is interpreted as IIIidvm1 (the muscle inserted to the precoxal bridge) by Friedrich & Beutel (2008), a muscle inserted to the trochantin should be interpreted as IIIidvm2 *sensu* Friedrich & Beutel (2008). There is no muscle corresponding to IIIidvm1 in the psocopteran metathorax.

4.2 | Phylogenetic significance of the thoracic muscles

The parsimony analysis of the thoracic muscle character data showed that this character system alone does not contain sufficient phylogenetic signal for resolving deep phylogeny of Psocodea. This is probably because, except for some homoplasious tiny muscles, most thoracic muscles are functionally constrained and thus are highly conservative within Psocodea.

The molecular/phylogenomic tree (Yoshizawa & Johnson, 2014; Johnson et al., 2018; de Moya et al., 2021) was identified as nearly optimal (length = 22, in compare to 21 for the most parsimonious tree) from the thoracic muscle character point of view. By parsimonious mapping of the thoracic muscle characters on the molecular/phylogenomic tree, several characters supporting the deep clades of Psocodea were newly identified.

The monophyly of Psocodea has been well supported morphologically, molecularly, and phylogenomically (e.g., Yoshizawa & Johnson, 2013; Beutel et al., 2014; Misof et al., 2014; Johnson et al., 2018). However, no thoracic muscle character supporting this order was identified.

The sister group relationship between the suborders Troctomorpha and Psocomorpha has long been assumed (e.g., Mockford, 1993; Lienhard, 1998) and has received strong support from molecular and phylogenomic analyses (Yoshizawa et al., 2006; Johnson et al., 2018; de Moya et al., 2021). In contrast, there are only a few apomorphic characters supporting this clade, such as a pair of character states observed in the wing coupling systems (Ogawa & Yoshizawa, 2018a,b). Now it is widely known that the phylogenomic dataset is not a panacea for elucidating phylogeny (e.g., Kumar et al., 2012), and some ambiguities or apparent errors are detected regarding the phylogenomics of Psocodea (Misof et al., 2014; Johnson et al., 2018; de Moya et al., 2021). Therefore, morphological data remain important to test or corroborate phylogenomic trees (Beutel et al., 2014). The present analysis newly identified two nonhomoplasious apomorphic conditions in the thoracic muscles supporting the sister group relationship between Troctomorpha and Psocomorpha (Figure 6). Now, the relationship receives morphological support from independent character systems so that, although Troctomorpha + Psocomorpha is already strongly supported molecularly, this relationship is now corroborated morphologically.

Support from the thoracic musculature for the suborders Trogiomorpha and Troctomorpha is ambiguous. A couple of character states may potentially support these suborders, but these are not unambiguously reconstructed on the tree (therefore, not shown in Figure 6). Character 1:0 provides support for Troctomorpha, but only one species was sampled from this suborder so that this might have evolved in a much shallower clade (family, genus or even species).

The monophyly of Psocomorpha is supported molecularly and phylogenomically (Yoshizawa & Johnson, 2014; Johnson et al., 2018; de Moya et al., 2021), and several morphological characters,

including nonhomoplasious ones, also support this suborder (Yoshizawa, 2002). The present analysis provided an additional apomorphy, fan-shaped II/IIItpm2. This character state is also observed in Aphididae (outgroup).

In contrast, no character informative for resolving the infraordinal relationships within Psocomorpha was detected, except for a single character supporting Epipsocetae + Psocetae. Although the infraordinal relationships are well resolved phylogenomically, no decisive morphological characters have been detected for them (e.g., Caeciliusetae + Homilopsocidea; Philotarsetae + Epipsocetae + Psocetae: Yoshizawa & Johnson, 2014). In particular, the thoracic musculatures of *Valenzuela* (Caeciliusetae) and *Heterocaecilius* (Philotarsetae) are similar, and no detectable difference between the species belonging to different clades was observed in the present examinations. The phylogenomic tree showed that, except for the split between Archipsocetae and the others, the divergence time of the psocomorphan infraorders is short (de Moya et al., 2021). Therefore, no useful apomorphy might have accumulated in slowly evolving thoracic muscles. Alternatively, rapidly evolving characters could be too noisy to resolve deep phylogeny. Morphological resolution of the psocomorphan higher-level phylogeny could present a difficult problem.

Because only one species was sampled for each infraorder (and for the suborder Troctomorpha), some characters detected at the terminal branches may contain phylogenetic signals at lower-level phylogeny. Although somewhat homoplasious, Character 1:0 was identified as an autapomorphy of Atropetae (Trogiomorpha), Troctomorpha, and Psocetae (Psocomorpha). The infraorder Psyllipsocetae of Trogiomorpha was not sampled in the present analyses, so this character state may support Psyllipsocetae + Atropetae (if the former also has this condition), which is also supported molecularly and phylogenomically (Yoshizawa et al., 2006; Johnson et al., 2018; de Moya et al., 2021). In contrast, it may also be possible that these apomorphies are specific for family, genus or even species. Further sampling will help to unambiguously identify the evolutionary history and phylogenetic signal of these character states.

Acknowledgments We thank Charles Lienhard for supplying valuable materials used in this study. Research at SPring-8 was approved through project numbers 2016A1269 (leader: Ryuichiro Machida), 2017B1712, 2018B1688, and 2018B1725 (leader: Naoki Ogawa). KY thanks Kentaro Uesugi for his support with the μ CT scanning and R. Machida for allowing KY and NO to join the SPring-8 project. This study was partly supported by JSPS Grant 19H03278 to KY and was partly conducted to fulfill AK's Bachelor's degree. The authors declared no conflict of interests.

REFERENCES

- Badonnel, A. (1934). Recherches sur l'Anatomie des Psocues. *Bulletin Biologique de France et de Belgique, Suppléments, 18*, 1–241.
- Beutel, R. G., Friedrich, F., Ge, S. Q., & Yang, X. K. (2014). *Insect Morphology and Phylogeny*. Berlin, Germany: De Gruyter GmbH.
- Brodsky, A. K. (1994). *The Evolution of Insect Flight* (pp. 1–299). Oxford, UK: Oxford University Press.
- Cope, O. B. (1940) The morphology of *Psocus confraternus* Banks (Psocoptera: Psocidae). *Microentomology, 5*, 91–115.
- Czihak, G. (1953) Beiträge zur Anatomie des Thorax von *Sialis flavilatera* L. *Österreichische Zoologische Zeitschrift, 4*, 421–448.
- de Moya, R., Yoshizawa, K., Walden, K. K. O., Sweet, A. D., Dietrich, C. H., & Johnson, K. P. (2021). Phylogenomics of parasitic and non-parasitic lice (Insecta: Psocodea): Combining sequence data and exploring compositional bias solution in Next Generation Datasets. *Systematic Biology, 70*, 719–738.
- Friedrich, F., & Beutel, R. G. (2008). The thorax of *Zorotypus* (Hexapoda, Zoraptera) and a new nomenclature for the musculature of Neoptera. *Arthropod Structure & Development, 37*, 29–54.
- Friedrich, F., & Beutel, R. G. (2010). The thoracic morphology of *Nannochorista* (Nannochoristidae) and its implications for the phylogeny of Mecoptera and Antiliphora. *Journal of Zoological Systematics and Evolutionary Research, 48*, 50–74.
- Johnson, K. P., Dietrich, C. H., Friedrich, F., Beutel, R. G., Wipfler, B. et al. (2018). Phylogenomics and the evolution of hemipteroid insects. *Proceedings of the National Academy of Science of the United States of America, 115*, 12775–12780.
- Kumar, S., Filipski, A. J., Battistuzzi, F. U., Kosakovsky Pond, S. L. & Tamura, K. (2012). Statistics and truth in phylogenomics. *Molecular Biology and Evolution, 29*, 457–472.
- Lienhard, C. (1998). Psocoptères Euro-Méditerranéens. *Faune de France, 83*, 1–517 + 11 plates.
- Maddison, D. R. & Maddison, W. P. (2001). *MacClade 4: Analysis of Phylogeny and Character Evolution*. Sunderland, UK: Sinauer Inc.
- Maki, T. (1936) Studies of the skeletal structure musculature and nervous system of the alder fly *Chauliodes formosanus* Peterson. *Memoires of the Faculty of Science and Agriculture Taihoku Imperial University, 16*, 117–243 + 10 plates.
- Maki, T. (1938) Studies on the thoracic musculature of insects. *Memoirs of the Faculty of Science and Agriculture Taihoku Imperial University, 24*, 1–343 + 11 plates.
- Misof, B., Liu, S., Meusemann, K., Peters, R. S., Donath, A., et al. (2014). Phylogenomics resolves the timing and pattern of insect evolution. *Science, 346*, 763–767.

- Mockford, E. L. (1993) *North American Psocoptera* (pp. 1–455). Gainesville, FL: Sandhill Crane Press.
- Ogawa, N., & Yoshizawa, K. (2018a) Origin and transformation of the in-flight wing-coupling structure in Psocodea (Insecta: Paraneoptera). *Journal of Morphology*, 279, 517–520.
- Ogawa, N., & Yoshizawa, K. (2018b). Structure and evolution of the stigmaphopysis – a unique repose wing-coupling structure in Psocodea. *Arthropod Structure & Development*, 47, 416–422.
- Snodgrass, R. E. (1935). *Principles of Insect Morphology*. Ithaca, NY: Cornell University Press.
- Swofford, D. L. (2002). *PAUP*: Phylogenetic Analysis Using Parsimony (* and other methods), version 4.0a*. Sunderland, UK: Sinauer Inc.
- Uesugi, K., Hoshino, M., Takeuchi, A., Suzuki, Y., Yagi, N. (2012). Development of fast and high throuput tomography using CMOS image detector at SPring-8. *Developments in X-Ray Tomography VIII*, 850601.
- Uesugi, K., Hoshino, M., & Takeuchi, A. (2017). Introducing high efficiency image detector to X-ray imaging tomography. *Journal of Physics: Conference Series*, 849, 012051.
- Yoshizawa, K. (2002). Phylogeny and higher classification of suborder Psocomorpha (Insecta: Psocodea: "Psocoptera"). *Zoological Journal of the Linnean Society*, 136, 371–400.
- Yoshizawa, K. (2005). Morphology of Psocomorpha (Psocodea: 'Psocoptera'). *Insecta Matsumurana, New Series*, 62, 1–44.
- Yoshizawa, K., & Johnson, K. P. (2014). Phylogeny fo the suborder Psocomorpha: Congruence and incongruence between morphology and molecular data (Insecta: Psocodea: "Psocoptera"). *Zoological Journal of the Linnean Society*, 171, 716–731.
- Yoshizawa, K., & Lienhard, C. (2016). Bridging the gap between chewing and sucking in the hemipteroid insects: New insights from Cretaceous amber. *Zootaxa*, 4079, 229–245.
- Yoshizawa, K., & Saigusa, T. (2001). Phylogenetic analysis of paraneopteran orders (Insecta: Neoptera) based on forewing base structure, with comments on monophyly of Auchenorrhyncha. *Systematic Entomology*, 26, 1–13.
- Yoshizawa, K., Lienhard, C., & Johnson, K. P. (2006). Molecular systematics of the suborder Trogiomorpha (Insecta: Psocodea: 'Psocoptera'). *Zoological Journal of the Linnean Society*, 146, 287–299.
- Yushkevich, P. A., Piven, J., Hazelett, H. C., Smith, R. G., Ho, S., Gee, J. C., & Gerig, G. (2006). User-guided 3D active contour segmentation of anatomical structures: Significantly improved efficiency and reliability. *NeuroImage*, 31, 1116–1128.

Figure Captions

Figure 1. 3D-reconstruction of the thoracic musculature (head to left, except for i) of (a–j) *Prionoglaris stygia* in (a)–(g) lateral view, (h) ventrolateral view, (i) posterior view, (j) posterolateral view; (k) Amphientomidae Gen. sp. in anterolateral view. Scale = 0.1 mm.

Figure 1. Continued.

Figure 1. Continued.

Figure 2. Postero-dorso-internal view (head to left) of mesothoracic dorso-ventral indirect flight muscles (IIdvm1 and IIdvm2) of (a) *Prionoglaris stygia* (one external dvm1 and one internal dvm2); (b) Amphientomidae Gen. sp. (no dvm1 and one dvm2); (c) *Archipsocus* sp. (two internal dvm1 and one external dvm2); (d) *Valenzuela* (two external dvm1 and one internal dvm2); (e) *Heterocaecilius solocipennis* (two external dvm1 and one internal dvm2); (f) *Epiopsocopsis* sp. (one anterior dvm1 and two posterior dvm2). Scale = 0.1 mm.

Figure 3. 3D model (a,c: head to left) and scanned image (b,d) of *Prionoglaris stygia* (a,b) and *Archipsocus* sp. (c,d), showing different conditions of IItpm1 and IItpm2 muscles. Scale = 0.1 mm.

Figure 4. 3D-model (a, c: head to left) and scanned image (b, d) of *Prionoglaris stygia* (a, b) and Amphientomidae Gen. sp. (c, d), showing the presence (a, b) and absence (c, d) of the IIsplm1 muscle. Scale = 0.1 mm.

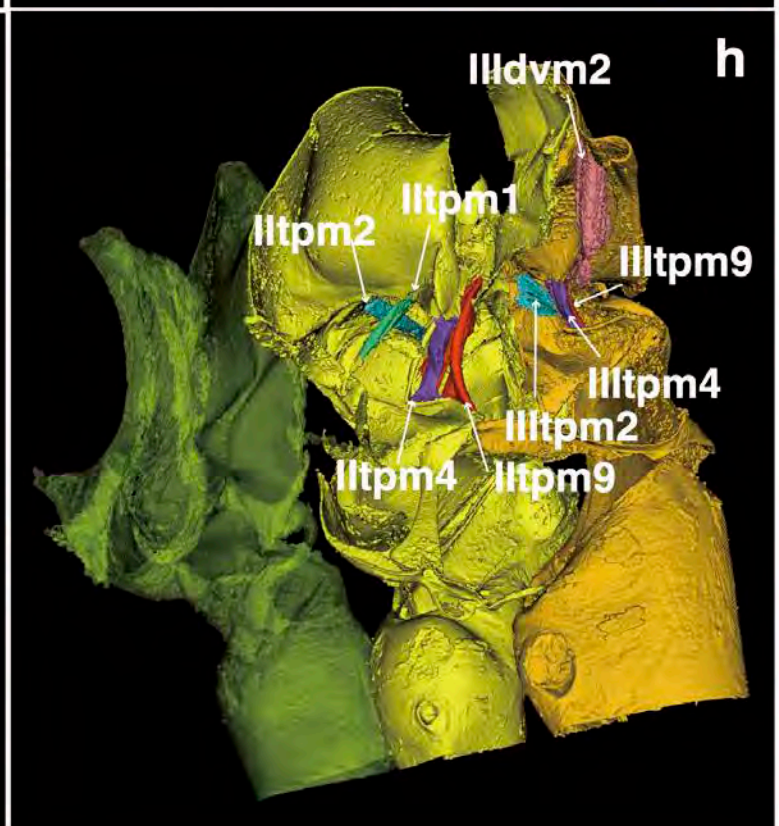
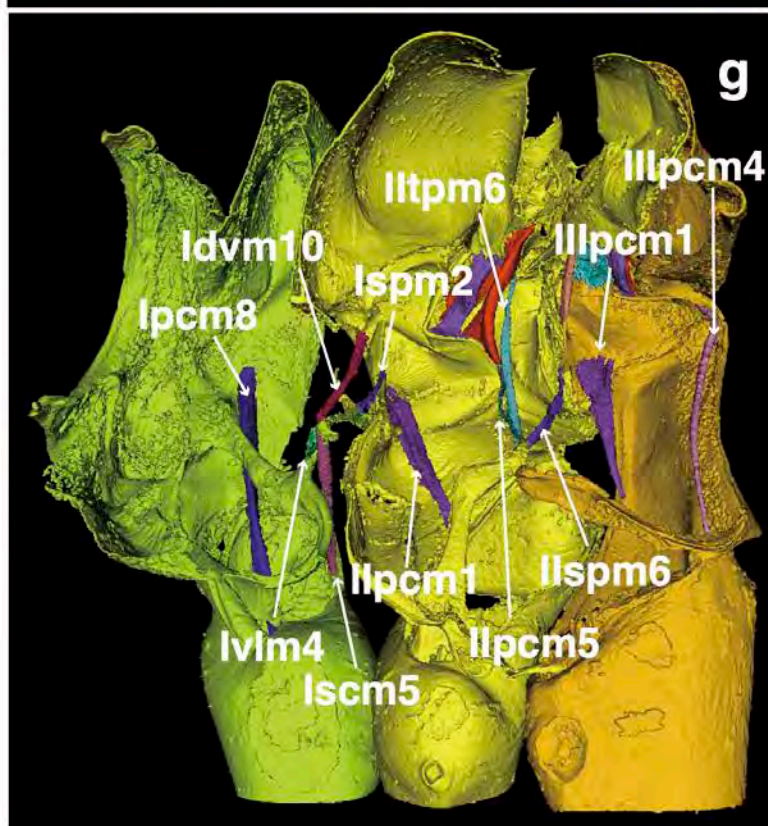
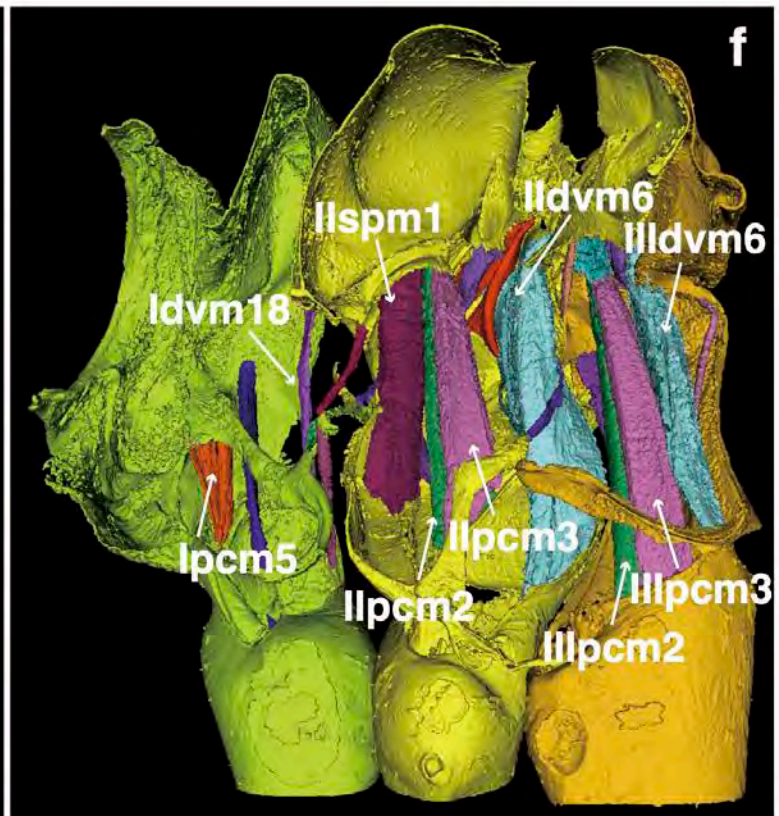
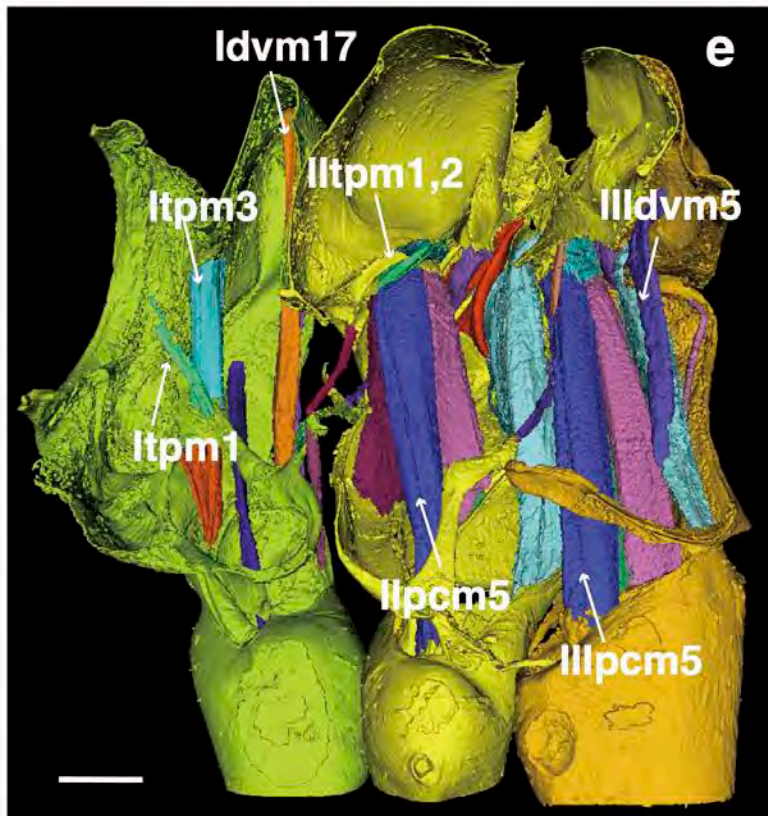
Figure 5. 3D-model (head to left) of (a,c) *Prionoglaris stygia* and (b,d) Amphientomidae Gen. sp.: (a,b) the presence (a) and absence (b) of IIsplm2; (c,d) the absence (c) and presence (d) of IIIpcm7. White arrowheads in b,c indicate the homologous position of the origin and insertion sites of the reduced muscles. Scale = 0.1 mm.

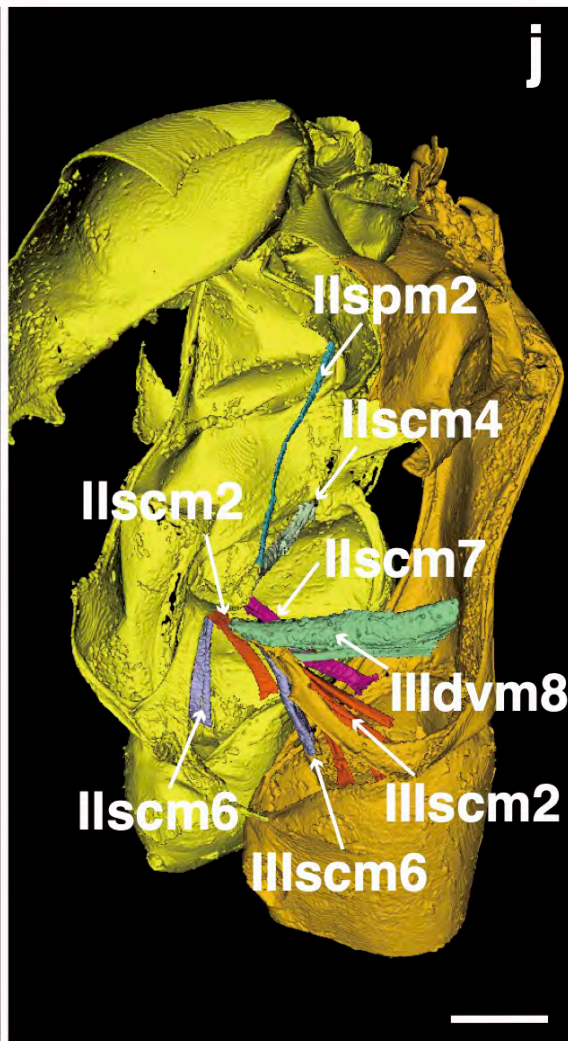
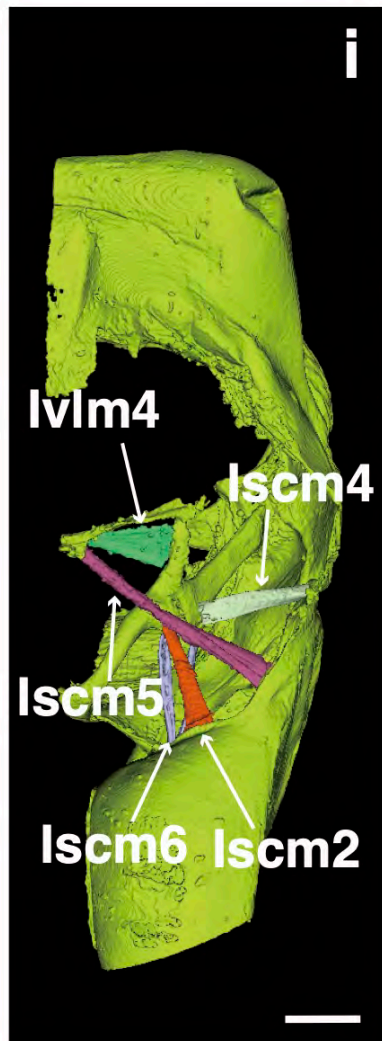
Figure 6. Phylogenetic relationships of the psocopteran taxa examined in this study and the most parsimonious reconstruction of the thoracic muscle characters detected in the present study.

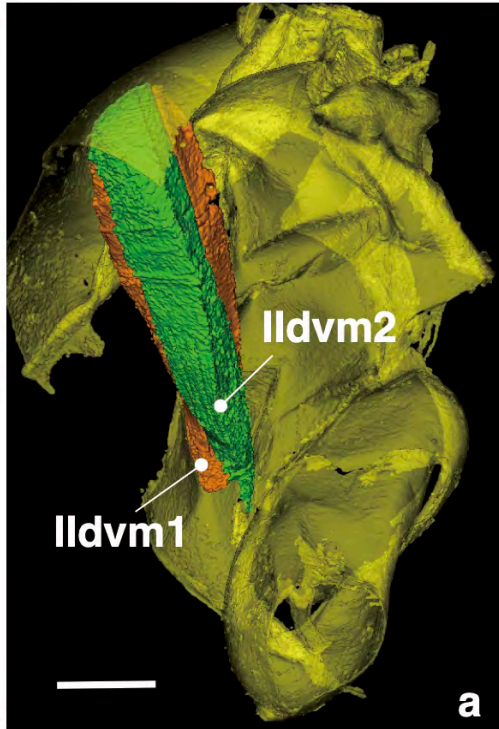
Abbreviations: Trog. = Trogiomorpha; Troc. = Troctomorpha.

Table 1. Taxa newly examined in this study. Data for the outgroup taxa are from Friedrich & Beutel (2008, 2012).

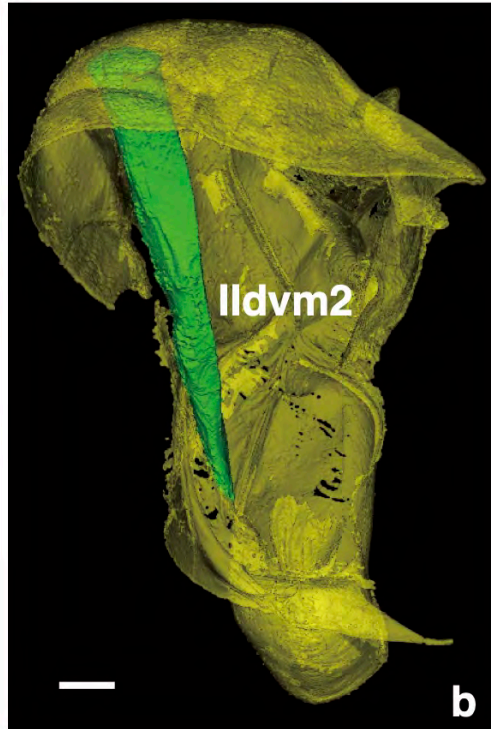
Table 2. Homologisation of the thoracic muscle nomenclatures used in the present study with those in Badonnel (1934) and Maki (1938).



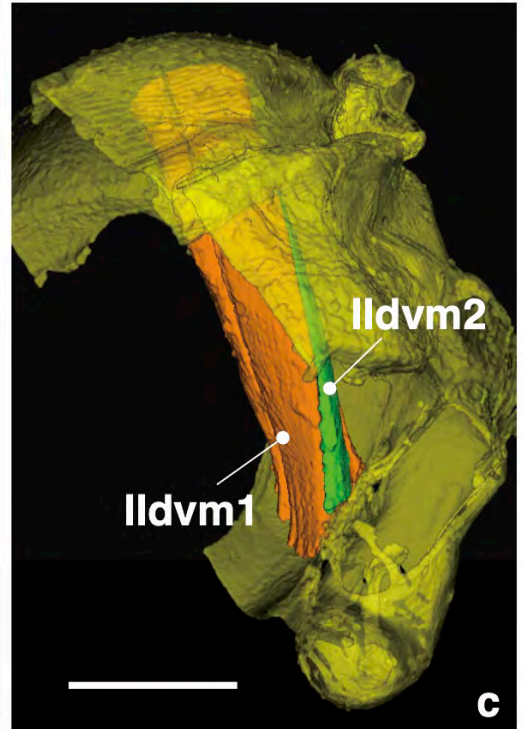




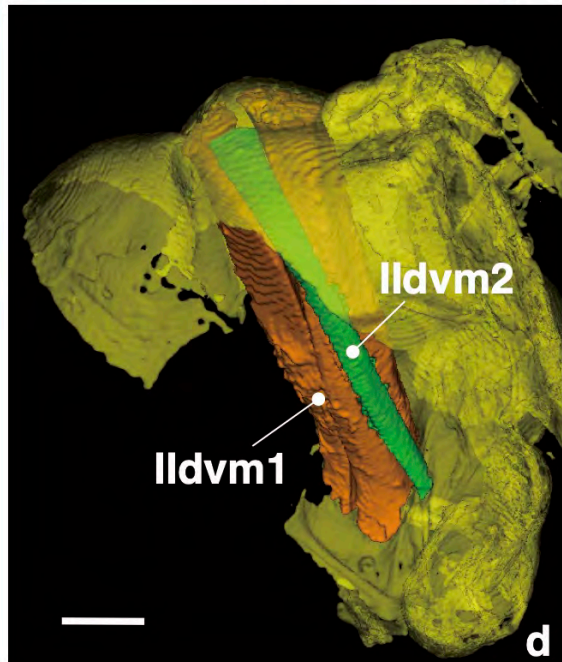
a



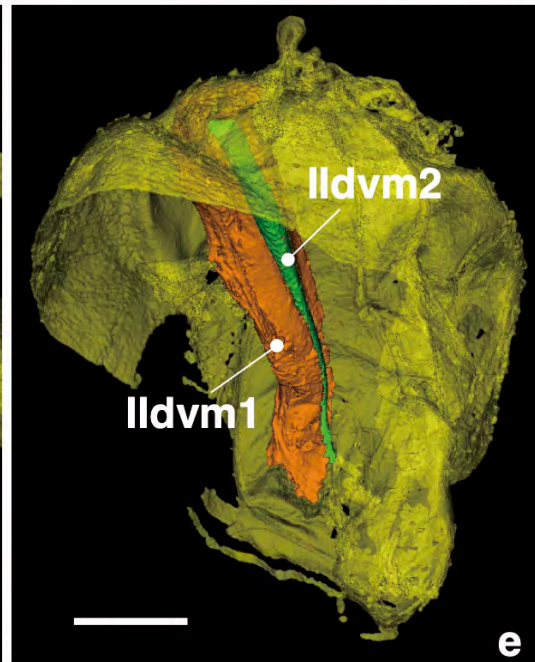
b



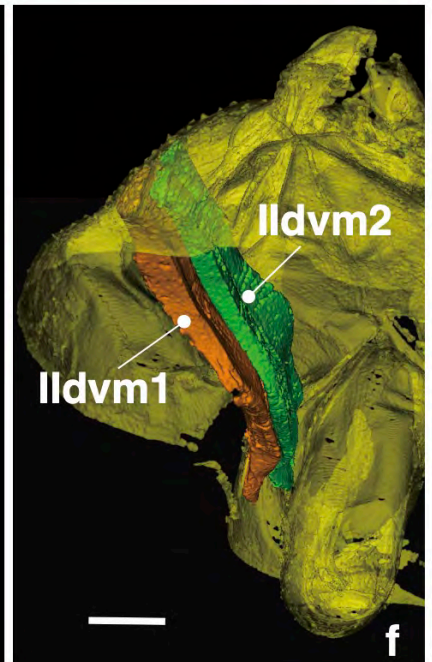
c



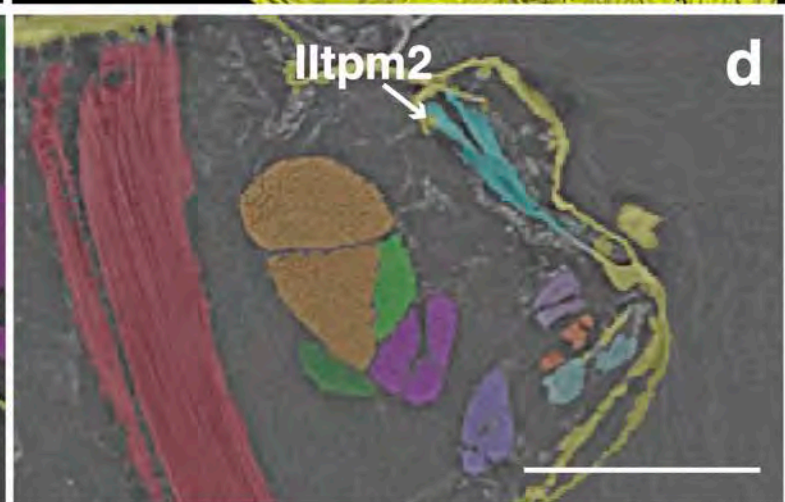
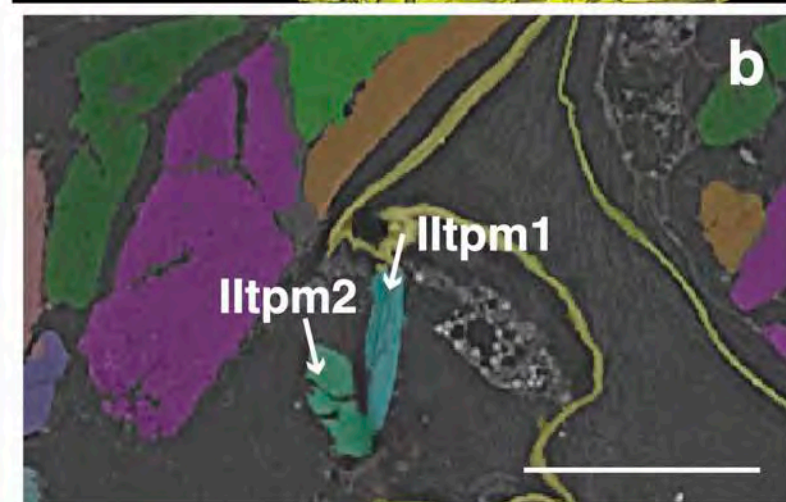
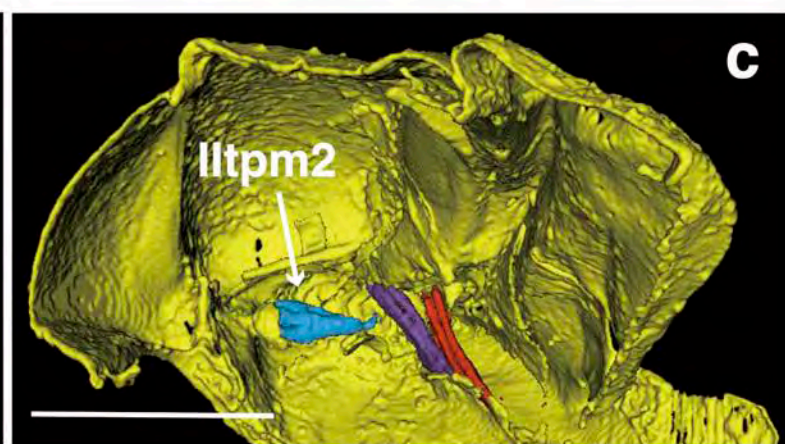
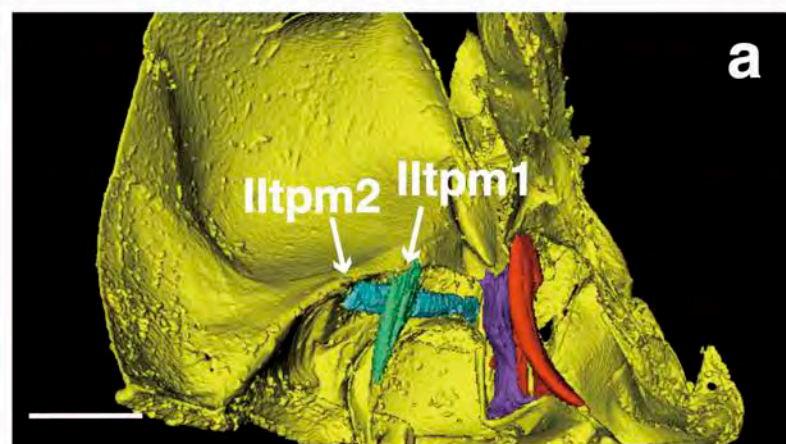
d

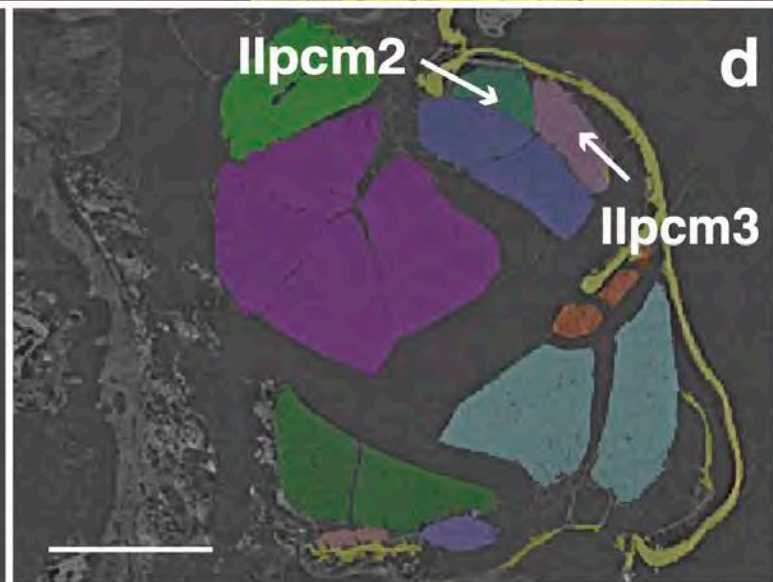
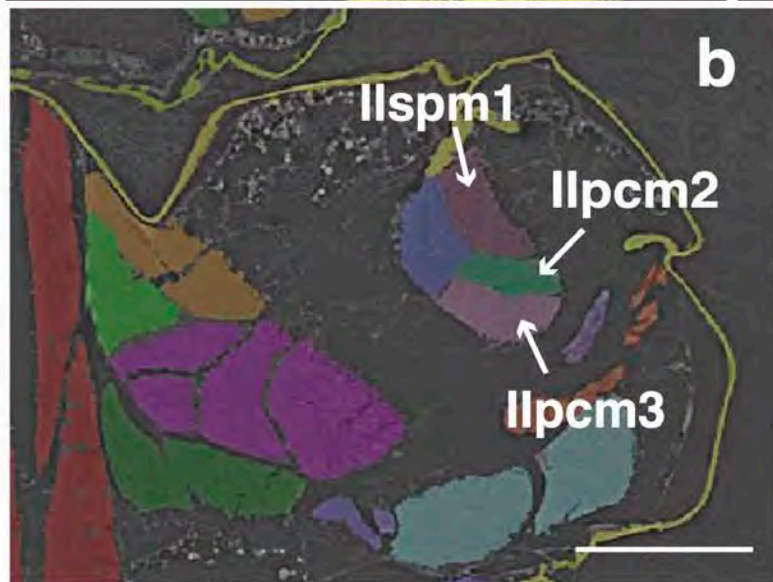
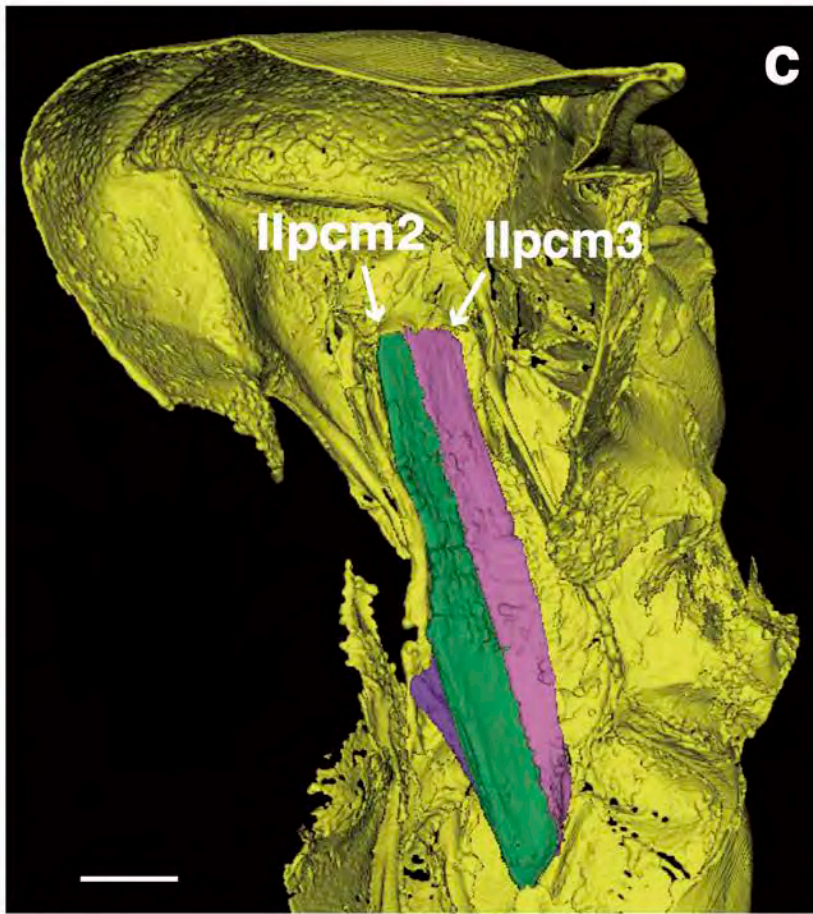
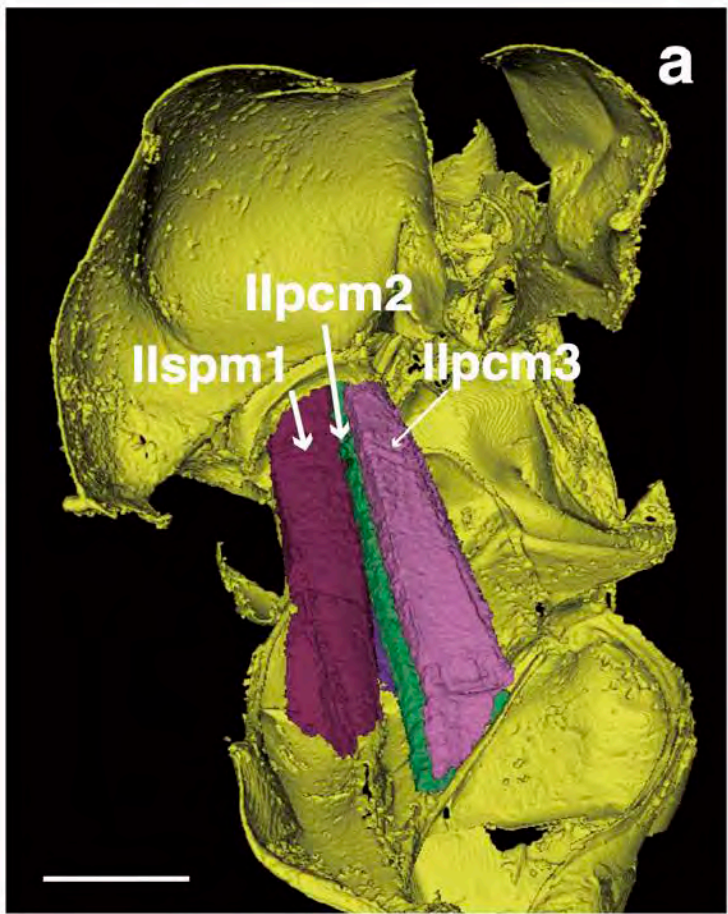


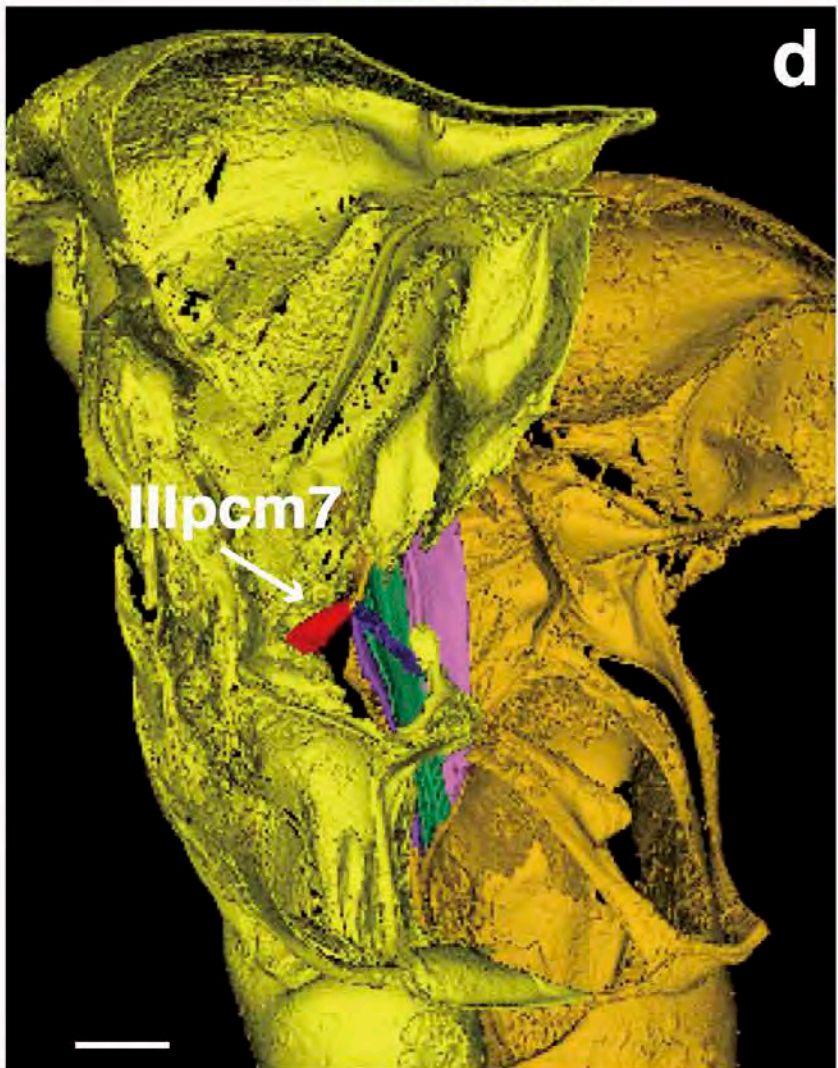
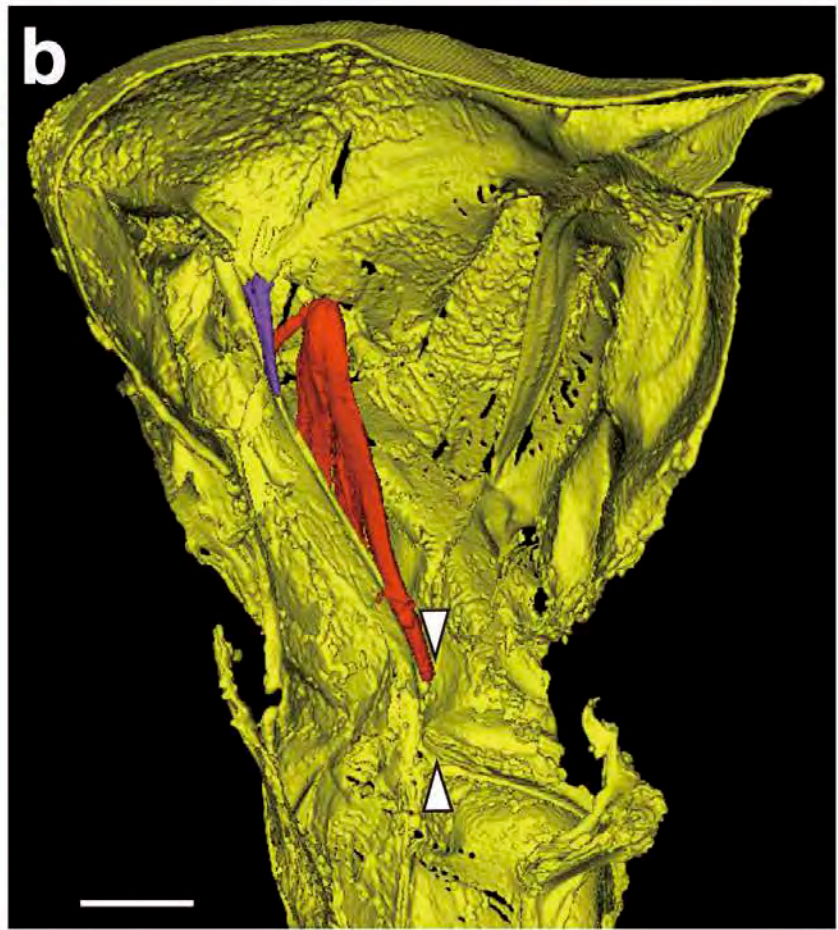
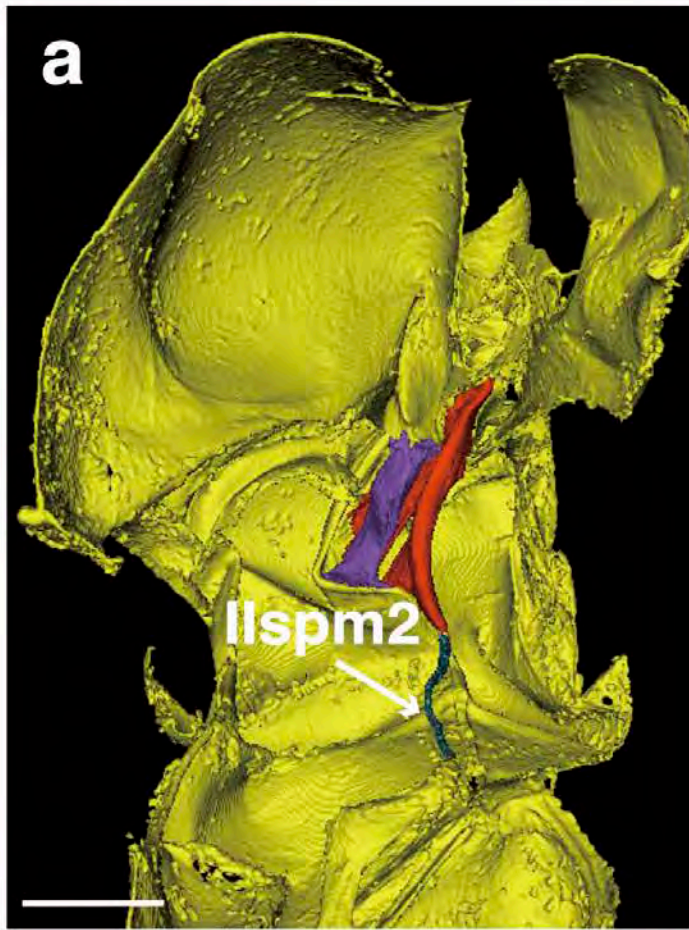
e



f







Zorotypidae

Mecoptera

Megaloptera

Aphididae

Trog.

Prionoglarididae

Atropetae

Troc.

Amphientometae

Archipsocetae

Caeciliusetae

Philotaesetae

Episocetae

Psocetae

Psocomorpha

3:1->0

6:1->0

9:0->1

1:
1->0

1:
1->0

6:1->0

9:0->1

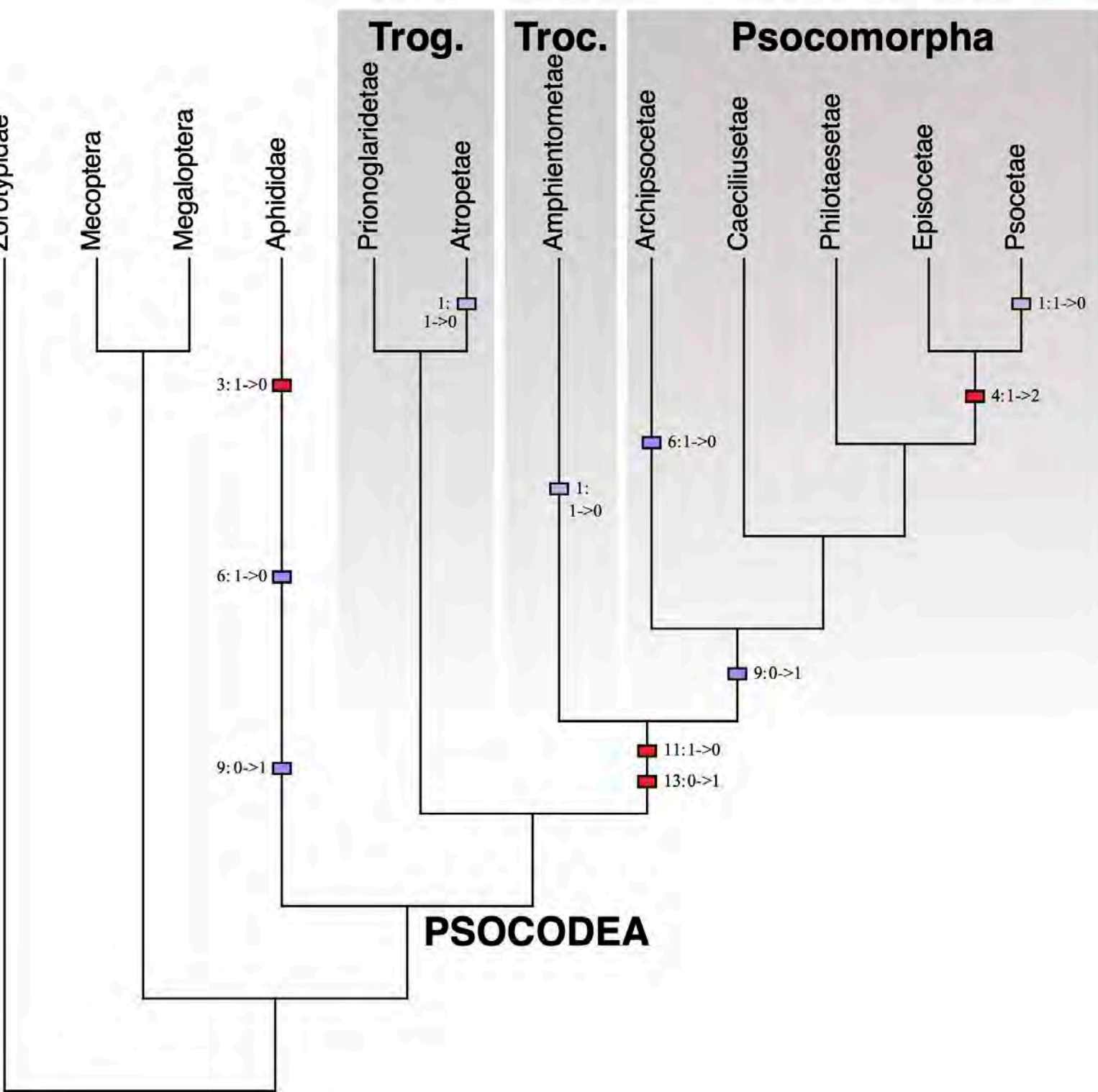
11:1->0

13:0->1

1:1->0

4:1->2

PSOCODEA



1					
2	Order	Suborder	Infraorder	Family	
3	Psocodea	Trogiomorpha	Prionoglaridetae	Prionoglarididae	
4			Atropetae	Lepidopsocidae	
5		Troctomorpha	Amphientometae	Amphientomidae	
6			Psocomorpha	Archipsocetae	Archipsocidae
7				Caeciliusetae	Caeciliusidae
8		Philotarsetae		Pseudocaeciliidae	
9		Epipsocetae		Epipsocidae	
10		Hemiptera	Sternorrhyncha	Psocetae	Psocidae
11				Aphidomorpha	Aphididae
12					
13					
14					
15					
16					
17					
18					
19					
20					
21					
22					
23					
24					
25					
26					
27					
28					
29					
30					
31					
32					
33					
34					
35					
36					
37					
38					
39					
40					
41					
42					
43					
44					
45					
46					
47					
48					
49					
50					
51					
52					
53					
54					
55					
56					
57					
58					
59					
60					

For Peer Review

Species	Specimen ID	Locality
<i>Prionoglaris stygia</i>	S8KY37	France
<i>Echmepteryx hageni</i>	S8KY84	Japan
Genus sp.	S8KY35	Malaysia
<i>Archipsocus</i> sp.	S8KY75	Mexico
<i>Valenzuela badiostigma</i>	S8KY19	Japan
<i>Heterocaecilius solocipennis</i>	S8KY18	Japan
<i>Epipsocopsis</i> sp.	S8KY76	Malaysia
<i>Trichadenotecnum circularoides</i>	CLKYtri	Japan
<i>Mindarus japonicus</i>	16aON12	Japan

For Peer Review

表1

Prothorax	Badonnel (1934)	Maki (1938)	Meso-	Badonnel (1934)	Maki (1938)	Meta-	Badonnel (1934)
ldlm1	DPo	(2)	lldlm1	DL	18	llldlm1	DL
ldlm2	DVL1	(2)	lldlm2	DO	19	llldlm2	DO
ldlm5	DPr	1	lldvm1	K	–	llldvm2	K
ldvm1	DVA	5	lldvm2	K'	29	llldvm5	I
ldvm2	DVL2	6	lldvm4	–	31	llldvm6	F
ldvm4	T	7	lldvm5	I	22	llldvm7	A
ldvm10	U	8	lldvm6	F	32	llldvm8	h3
ldvm15	L	12	lldvm7	A	39	llltpm2	Z
ldvm16	–	14	lltpm1	–	23?, 24	llltpm4	W2,3
ldvm17	C	–	lltpm2	Z	25	llltpm9	W1
ldvm18	F	–	lltpm4	W2,3	26,27	lllpcm1	e
ldvm19	A	.0.	lltpm 6	–	–	lllpcm2	–
ltpm1	LL	9	lltpm9	W1	28	lllpcm3	E
ltpm3	G	10	llspm1	–	–	lllpcm4	e'
lspm2	h2	–	lisp2	–	–	lllpcm5	A'
lpcm2	X1	13	llspm6	U	–	lllpcm7	H
lpcm5	E	16	llpcm1?	e	–	lllscm2	J
lpcm8	A'	–	llpcm2	E	33	lllscm6	m
lvim3	LV1	3	llpcm3	E	34		
lvim4	d1,2	4	llpcm5	e'	38,40		
lvim6	LVL2	21	llvim3	LVI3, LVL3	45		
lvim7	LVI2	20	llscm2	J	35		
lvim9	LVM2	–	llscm4	Y	–		
lscm1	m	–	llscm6	m	41		
lscm4	–	15	llscm7	X3	–		
lscm5	J	–					
lscm6	a	11					
lscm7	X2	30					

